Theoretical and Applied Climatology (2022) 149:15–24
https://doi.org/10.1007/s00704-022-04022-7

ORIGINAL PAPER

Analysis of the July 2021 extreme precipitation in Henan using the novel moisture budget equation

Jianbo Cheng[1] · Yuheng Zhao[2] · Rong Zhi[1,2] · Guolin Feng[3,4]

Received: 14 December 2021 / Accepted: 17 March 2022 / Published online: 30 March 2022

Abstract

In this study, we use the moisture budget equation and the three-pattern decomposition of global atmospheric circulation to analyze the extreme precipitation in Henan Province that occurred from 17 to 22 July 2021. The results obtained from the moisture budget equation show that the dynamic and thermodynamic terms can explain 75% and 22% of the anomalous precipitation, respectively, while the residual term only explains 3%. Changes in divergence (advection) are the main contributor to the dynamic (thermodynamic) term, which can explain 80% (22%) of the anomalous precipitation. Further analysis based on the novel moisture budget equation shows that the contributions of the horizontal, meridional, and zonal circulations to the anomalous precipitation caused by the dynamic term induced by divergence and thermodynamic term induced by advection are 13%, 13%, and 76%, respectively, suggesting the dominant role of zonal circulation in causing this anomalous precipitation. The underlying physical mechanism of horizontal, meridional, and zonal circulations in causing this anomalous precipitation was also studied.

1 Introduction

An extremely rare heavy rainstorm occurred in Henan Province from 17 to 22 July 2021; it exhibited significant extremes in terms of duration, heavy rainfall coverage, cumulative rainfall amount, and daily and hourly rainfall intensity (Shi et al. 2021; Sun et al. 2021; Zhang et al. 2021; Yin et al. 2021). According to statistics by the National Meteorological Center of China Meteorological Administration, the cumulative rainfall in most north-central regions of Henan Province exceeds 500 mm, and the region with accumulated rainfall greater than 250 mm accounts for 32.5% of the total land area of the province. Particularly, the cumulative rainfall reached 993.1 mm at the meteorological station of Baizhai town in Zhengzhou city and 1122.6 mm at the meteorological station of the Science and Technology Center in Hebi city. The daily rainfall exceeded 100 mm for approximately half of the meteorological stations and exceeded the historical maximum for twenty national meteorological stations in Henan Province. Particularly, the maximum daily rainfall recorded by the national meteorological station of Zhengzhou reached 624.1 mm, which is 3.3 times the historical maximum daily rainfall. Due to heavy rainfall disasters, extraordinary floods occurred in various cities and regions of Henan Province, resulting in critical economic and social losses (Shi et al. 2021; Sun et al. 2021; Zhang et al. 2021; Yin et al. 2021). Particularly, 302 people died, 50 people were reported missing, and the direct economic loss has exceeded one hundred billion yuan (Shi et al. 2021). Therefore, the underlying causes of this extremely rare heavy rainfall in Henan Province should be investigated.

Regarding the critical socio-economic losses of this extreme precipitation, many efforts have been made to investigate the underlying causes. For example, Shi et al. (2021) suggested that the extreme precipitation was caused by the enhanced easterly jet, which was induced by the generation of typhoon "In-fa" and westwards extending of subtropical high. Zhang et al. (2021) claimed that the anomalous precipitation was closely related to topography. Sun et al. (2021) proposed that the rapid

✉ Rong Zhi
z_rongphy@126.com

✉ Guolin Feng
fenggl@cma.gov.cn

[1] School of Environmental Science and Engineering, Yancheng Institute of Technology, Yancheng, China

[2] Laboratory for Climate Studies, National Climate Center, China Meteorological Administration, Beijing, China

[3] College of Physical Science and Technology, Yangzhou University, Yangzhou, China

[4] Southern Marine Science and Engineering Guangdong Laboratory (Zhuhai), Zhuhai, China

enhancement of the anomalous precipitation was caused by transportation of hydrometeors into the uplifting zone of large-scale precipitation system. However, the analysis from the perspective of moisture budget has not been conducted. According to previous studies (Seager et al. 2010; Seager and Vecchi 2010; Han et al. 2019a, b, 2020; Qiao et al. 2021), the moisture budget equation can be written as $\delta P \approx \delta\mathrm{MCD} + \delta\mathrm{TH} + \delta R$, where δP is the anomalous precipitation, δMCD is the dynamic term, δTH is the thermodynamic term, and δR includes the contributions of anomalous evaporation, high-frequency variability of transient eddies, nonlinear effects, and surface boundary terms. The moisture budget equation shows that anomalous precipitation can be decomposed into the contributions of the dynamic term, thermodynamic term, and residual terms. Thus, the quantitative contributions of these terms on the right hand of the moisture budget equation to the extremely rare heavy rainfall in Henan Province in July 2021 can be investigated.

Although the quantitative contributions can be investigated from the perspective of the moisture budget, the underlying physical mechanism cannot be clearly clarified by the moisture budget equation. Fortunately, a novel three-pattern decomposition of the global atmospheric circulation (3P-DGAC) method has been developed to investigate the complex interactions of atmospheric circulations between low latitudes and middle–high latitudes (Liu et al. 2008; Hu et al. 2017, 2018a, b, 2020; Cheng et al. 2018). Hu et al. (2017) proposed that the global atmospheric circulation can be decomposed into the sum of the horizontal, meridional, and zonal circulations, which can be viewed as the global generation of the Rossby wave in the middle–high latitudes and the Hadley and Walker circulations in the low latitudes. Han et al. (2021) combined the 3P-DGAC method and the moisture budget equation to develop a novel moisture budget equation of three-pattern circulations. By using this novel moisture budget equation, the relative contributions of horizontal, meridional, and zonal circulations to extremely rare heavy rainfall and the underlying physical mechanism can be explored.

In this study, we aim to analyze the extreme precipitation in Henan Province from 17 to 22 July 2021 by using the moisture budget equation and the 3P-DGAC method. The remainder of this paper is organized as follows. Section 2 provides the data and methods used in this study. In Sect. 3, we investigate the quantitative contributions of the terms on the right side of the moisture budget equation to extreme rainfall. The relative contributions of the horizontal, meridional, and zonal circulations to extreme rainfall and the underlying physical mechanism are also explored. Finally, a summary is provided in Sect. 4.

2 Data and methods

2.1 Data

In this study, we use hourly rainfall data and associated atmospheric variables, including horizontal wind, vertical velocity, specific humidity, and surface pressure, derived from the European Center for Medium Range Weather Forecasts Reanalysis 5 (ERA5, Hersbach et al. 2020) with a horizontal resolution of $0.5° \times 0.5°$. The time period analyzed in this study is from 17 to 22 July in 2021, and the climatological mean of variables is defined as the climatological mean from 1981 to 2010.

2.2 Novel moisture budget equation of three-pattern circulations

In this study, the following moisture budget equation is adopted (Seager et al. 2010; Seager and Vecchi 2010):

$$\delta P \approx -\frac{1}{\rho_w g}\int_0^{p_s} \nabla\cdot\left(\vec{V}_0\delta q\right)dp - \frac{1}{\rho_w g}\int_0^{p_s} \nabla\cdot\left(q_0\delta\vec{V}\right)dp + \delta R \tag{1}$$

where ρ_w is the density of water, g is the gravitational acceleration, $\vec{V}$ is the horizontal wind, q is the specific humidity, p is the pressure, and p_s is the surface pressure. δ is the difference in variables between the period of 17 July to 22 July 2021 and the climatological mean of 1981–2010. Variables with subscript 0 represent the climatological mean of 1981–2010. $\delta\mathrm{TH} = -\frac{1}{\rho_w g}\int_0^{p_s} \nabla\cdot\left(\vec{V}_0\delta q\right)dp$ is the thermodynamic term that is induced by anomalous specific humidity. The thermodynamic term can further be decomposed into two components, i.e., $\delta\mathrm{TH} = \delta\mathrm{THA} + \delta\mathrm{THD} = -\frac{1}{\rho_w g}\int_0^{p_s}\left(\vec{V}_0\cdot\nabla\delta q\right)dp - \frac{1}{\rho_w g}\int_0^{p_s}\left(\delta q\nabla\cdot\vec{V}_0\right)dp$, where δTHA and δTHD represent the thermodynamic term induced by advection and divergence, respectively. $\delta\mathrm{MCD} = -\frac{1}{\rho_w g}\int_0^{p_s}\nabla\cdot\left(q_0\delta\vec{V}\right)dp$ is the dynamic term that is induced by anomalous circulation. The dynamic term can be decomposed into two components, i.e., $\delta MCD = \delta\mathrm{MCDA} + \delta\mathrm{MCDD} = -\frac{1}{\rho_w g}\int_0^{p_s}\left(\delta\vec{V}\cdot\nabla q_0\right)dp - \frac{1}{\rho_w g}\int_0^{p_s}\left(q_0\nabla\cdot\delta\vec{V}\right)dp$, where δMCDA and δMCDD represent the dynamic term induced by advection and divergence, respectively. The residual term δR includes the contributions of anomalous evaporation, high-frequency variability of transient eddies, nonlinear effects, and surface boundary terms.

The 3P-DGAC method (Liu et al. 2008; Hu et al. 2017, 2018a, b, 2020; Cheng et al. 2018) can be used to decompose the global atmospheric circulation $\vec{V}$ into the sum of the horizontal circulation $\vec{V}_H = u_H\vec{i} + v_H\vec{j}$, meridional circulation $\vec{V}_M = v_M\vec{j} + \omega_M\vec{k}$, and zonal circulation $\vec{V}_Z = u_Z\vec{i} + \omega_Z\vec{k}$, i.e.,

$$\vec{V} = \vec{V}_H + \vec{V}_M + \vec{V}_Z \tag{2}$$

with the following components:

$$\begin{cases} u = u_Z + u_H = a\left(p_s\frac{\partial Z}{\partial p} - \frac{\partial H}{\partial \theta}\right) \\ v = v_H + v_M = a\left(\frac{1}{sin\theta}\frac{\partial H}{\partial \lambda} - p_s\frac{\partial M}{\partial p}\right) \\ \omega = \omega_M + \omega_Z = \frac{p_s}{sin\theta}\frac{\partial (sin\theta M)}{\partial \theta} - \frac{p_s}{sin\theta}\frac{\partial Z}{\partial \lambda} \end{cases} \tag{3}$$

where a is the Earth radius and H, M, and Z are the stream functions of horizontal, meridional, and zonal circulations, respectively.

Han et al. (2021) combined the 3P-DGAC method and the moisture budget equation to develop a novel moisture budget equation of three-pattern circulations. Specifically, by combining Eqs. (1) and (3), the novel moisture budget equation of three-pattern circulations can be obtained as follows:

$$\begin{aligned} \delta P \approx & -\frac{1}{\rho_w g}\int_0^{p_s}\nabla\cdot(\vec{V}_{H0}\delta q)dp - \frac{1}{\rho_w g}\int_0^{p_s}\nabla\cdot(q_0\delta\vec{V}_H)dp \\ & -\frac{1}{\rho_w g}\int_0^{p_s}\nabla\cdot(\vec{V}_{M0}\delta q)dp - \frac{1}{\rho_w g}\int_0^{p_s}\nabla\cdot(q_0\delta\vec{V}_M)dp \\ & -\frac{1}{\rho_w g}\int_0^{p_s}\nabla\cdot(\vec{V}_{Z0}\delta q)dp - \frac{1}{\rho_w g}\int_0^{p_s}\nabla\cdot(q_0\delta\vec{V}_Z)dp + \delta R \end{aligned} \tag{4}$$

where $\delta\mathrm{TH\_H} = -\frac{1}{\rho_w g}\int_0^{p_s}\nabla\cdot\left(\overline{V}_{H0}\delta q\right)dp$ and $\delta\mathrm{MCD\_H} = -\frac{1}{\rho_w g}\int_0^{p_s}\nabla\cdot\left(q_0\delta\overline{V}_H\right)dp$ are the thermodynamic term and dynamic term induced by horizontal circulation, respectively; $\delta\mathrm{TH\_M} = -\frac{1}{\rho_w g}\int_0^{p_s}\nabla\cdot\left(\overline{V}_{M0}\delta q\right)dp$ and $\delta\mathrm{MCD\_M} = -\frac{1}{\rho_w g}\int_0^{p_s}\nabla\cdot\left(q_0\delta\overrightarrow{V}_M\right)dp$ are the thermodynamic term and dynamic term induced by meridional circulation, respectively; and $\delta\mathrm{TH\_Z} = -\frac{1}{\rho_w g}\int_0^{p_s}\nabla\cdot\left(\overrightarrow{V}_{Z0}\delta q\right)dp$ and $\delta\mathrm{MCD\_Z} = -\frac{1}{\rho_w g}\int_0^{p_s}\nabla\cdot\left(q_0\delta\overrightarrow{V}_Z\right)dp$ are the thermodynamic term and dynamic term induced by zonal circulation, respectively.

Furthermore, the thermodynamic term induced by the three-pattern circulations can be decomposed into the thermodynamic term induced by advection and divergence. Namely,

$$\begin{cases} \delta\mathrm{TH\_H} = \delta\mathrm{THA\_H} + \delta\mathrm{THD\_H} = -\frac{1}{\rho_w g}\int_0^{p_s}(\vec{V}_{H0}\cdot\nabla\delta q)dp - \frac{1}{\rho_w g}\int_0^{p_s}(\delta q\nabla\cdot\vec{V}_{H0})dp \\ \delta\mathrm{TH\_M} = \delta\mathrm{THA\_M} + \delta\mathrm{THD\_M} = -\frac{1}{\rho_w g}\int_0^{p_s}(\vec{V}_{M0}\cdot\nabla\delta q)dp - \frac{1}{\rho_w g}\int_0^{p_s}(\delta q\nabla\cdot\vec{V}_{M0})dp \\ \delta\mathrm{TH\_Z} = \delta\mathrm{THA\_Z} + \delta\mathrm{THD\_Z} = -\frac{1}{\rho_w g}\int_0^{p_s}(\vec{V}_{Z0}\cdot\nabla\delta q)dp - \frac{1}{\rho_w g}\int_0^{p_s}(\delta q\nabla\cdot\vec{V}_{Z0})dp \end{cases} \tag{5}$$

where δTHA_H, δTHA_M, and δTHA_Z (δTHD_H, δTHD_M, and δTHD_Z) represent contributions of the change in advection (divergence) to the thermodynamic term induced by the horizontal, meridional, and zonal circulations, respectively. Similarly, the dynamic term induced by the three-pattern circulations can be decomposed into the dynamic term induced by advection and divergence. Namely,

$$\begin{cases} \delta\mathrm{MCD\_H} = \delta\mathrm{MCDA\_H} + \delta\mathrm{MCDD\_H} = -\frac{1}{\rho_w g}\int_0^{p_s}(\delta\vec{V}_H\cdot\nabla q_0)dp - \frac{1}{\rho_w g}\int_0^{p_s}(q_0\nabla\cdot\delta\vec{V}_H)dp \\ \delta\mathrm{MCD\_M} = \delta\mathrm{MCDA\_M} + \delta\mathrm{MCDD\_M} = -\frac{1}{\rho_w g}\int_0^{p_s}(\delta\vec{V}_M\cdot\nabla q_0)dp - \frac{1}{\rho_w g}\int_0^{p_s}(q_0\nabla\cdot\delta\vec{V}_M)dp \\ \delta\mathrm{MCD\_Z} = \delta\mathrm{MCDA\_Z} + \delta\mathrm{MCDD\_Z} = -\frac{1}{\rho_w g}\int_0^{p_s}(\delta\vec{V}_Z\cdot\nabla q_0)dp - \frac{1}{\rho_w g}\int_0^{p_s}(q_0\nabla\cdot\delta\vec{V}_Z)dp \end{cases} \tag{6}$$

where δMCDA_H, δMCDA_M, and δMCDA_Z (δMCDD_H, δMCDD_M, and δMCDD_Z) represent contributions of the change in advection (divergence) to the dynamic term induced by the horizontal, meridional, and zonal circulations, respectively.

By using the novel moisture budget equation of the three-pattern circulation and Eqs. (5) and (6), the relative contributions of the horizontal, meridional, and zonal circulations to the extremely rare heavy rainfall and the underlying physical mechanism can be investigated.

3 Results

Figure 1a shows that the accumulated precipitation center between 17 and 22 July in 2021 from ERA5 reanalysis datasets is located around southern Shanxi, northern Henan, and western Hebei. The location and intensity of the precipitation anomaly center are similar to those of the precipitation center (comparing Fig. 1a,c), implying that the precipitation in 2021 is clearly stronger than the climatological precipitation from 1981 to 2010 (comparing Fig. 1a,b). Figure 2 displays the changes in the moisture budget components of 2021 minus the climatological mean (1981–2010), which reflect the sum of dynamic and thermodynamic terms (δMCD and δTH), the dynamic term (δMCD), and the thermodynamic term (δTH), the contributions of changes in divergence (δMCDD) and advection (δMCDA) to the dynamic term, and the contributions of changes in divergence (δTHD) and advection (δTHA) to the thermodynamic term. Figures 1c and 2a show that the spatial distribution of the sum of δMCD and δTH is similar to that of the precipitation anomaly in the region where extreme precipitation occurs (purple box in figure; 111°E–115°E, 33°N–39°N). The quantitative results in Fig. 4a show that the sum of dynamic and thermodynamic terms (121.7 mm) can explain 97% of the anomalous precipitation (125.5 mm), while the

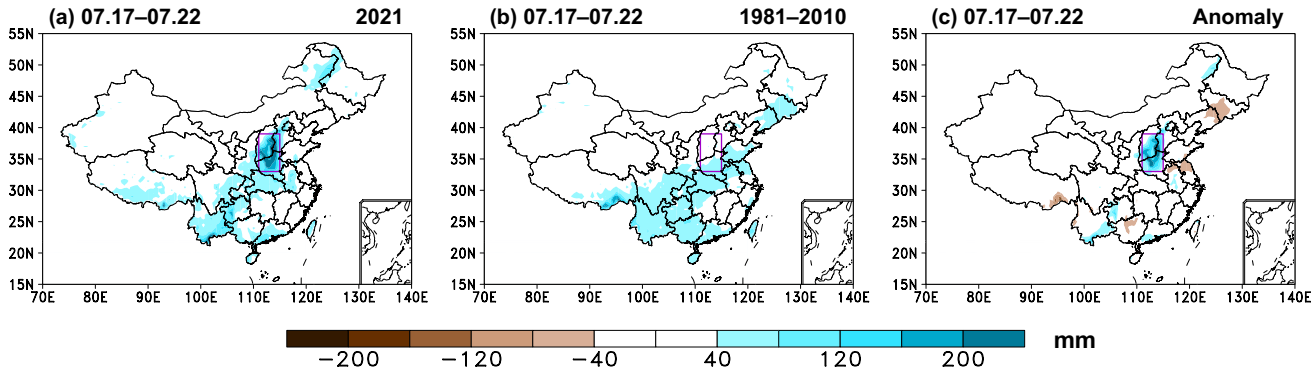

Fig. 1 **a** Spatial distribution of the accumulated precipitation from 17 to 22 July in 2021. (**b**) and (**c**) Same as (**a**) except for the climatological precipitation (1981–2010) and the precipitation anomaly in 2021. The purple box (111°E–115°E, 33°N–39°N) indicates the region where extreme precipitation occurs. The precipitation anomaly is computed based on the climatological mean of 1981–2010. The units for the precipitation and precipitation anomalies are mm

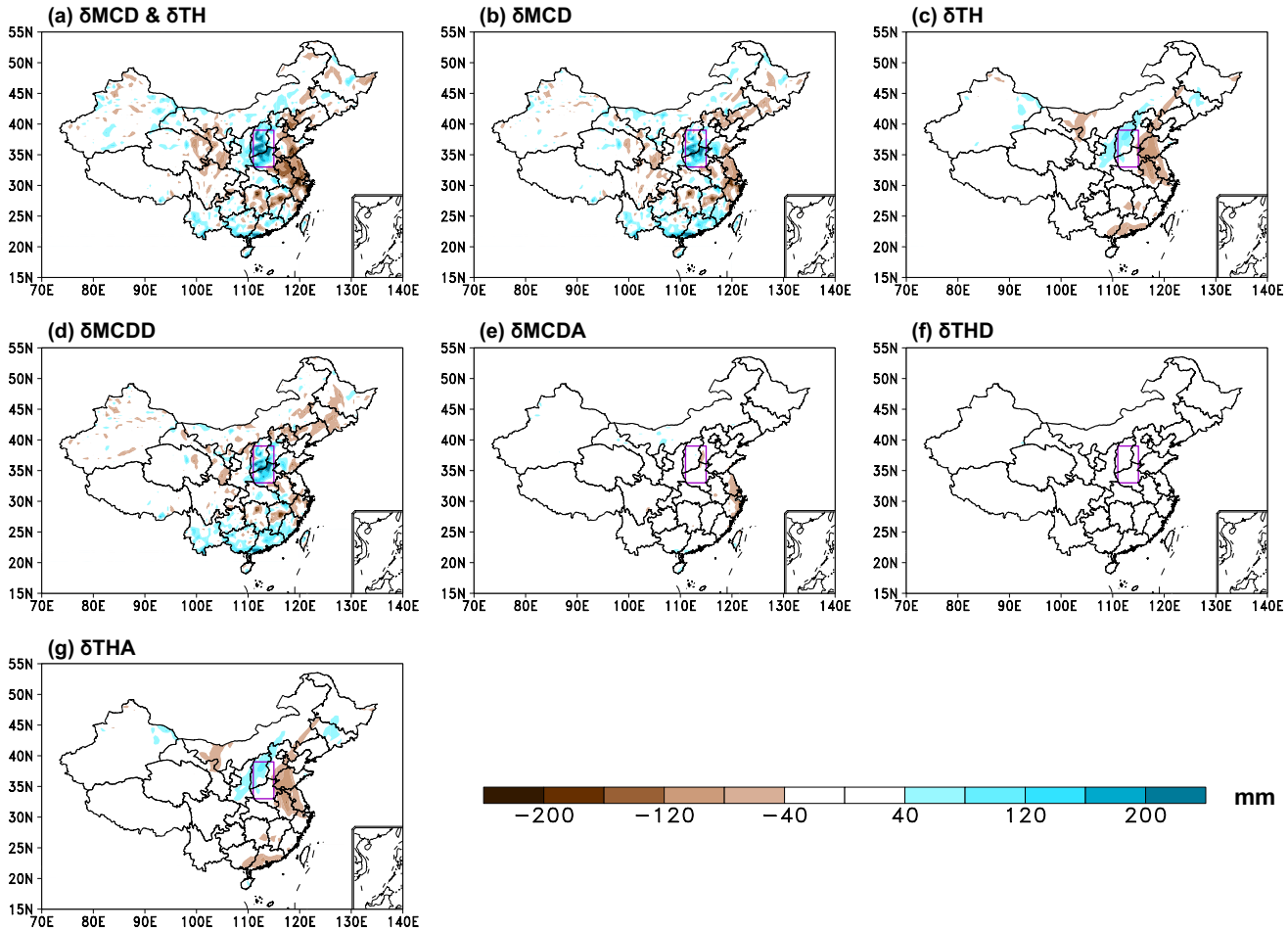

Fig. 2 The mean (from 17 to 22 July) changes in the moisture budget components of 2021 minus the climatological mean (1981–2010), which reflects (**a**) the dynamic and thermodynamic terms (δMCD and δTH), (**b**) the dynamic term (δMCD), and (**c**) the thermodynamic term (δTH). (**d**) and (**e**) Same as (**b**) except for the contributions of changes in divergence (δMCDD) and advection (δMCDA) to the dynamic term. (**f**) and (**g**) Same as (**c**) except for the contributions of changes in divergence (δTHD) and advection (δTHA) to the thermodynamic term. The units for the changes in the moisture budget components are mm

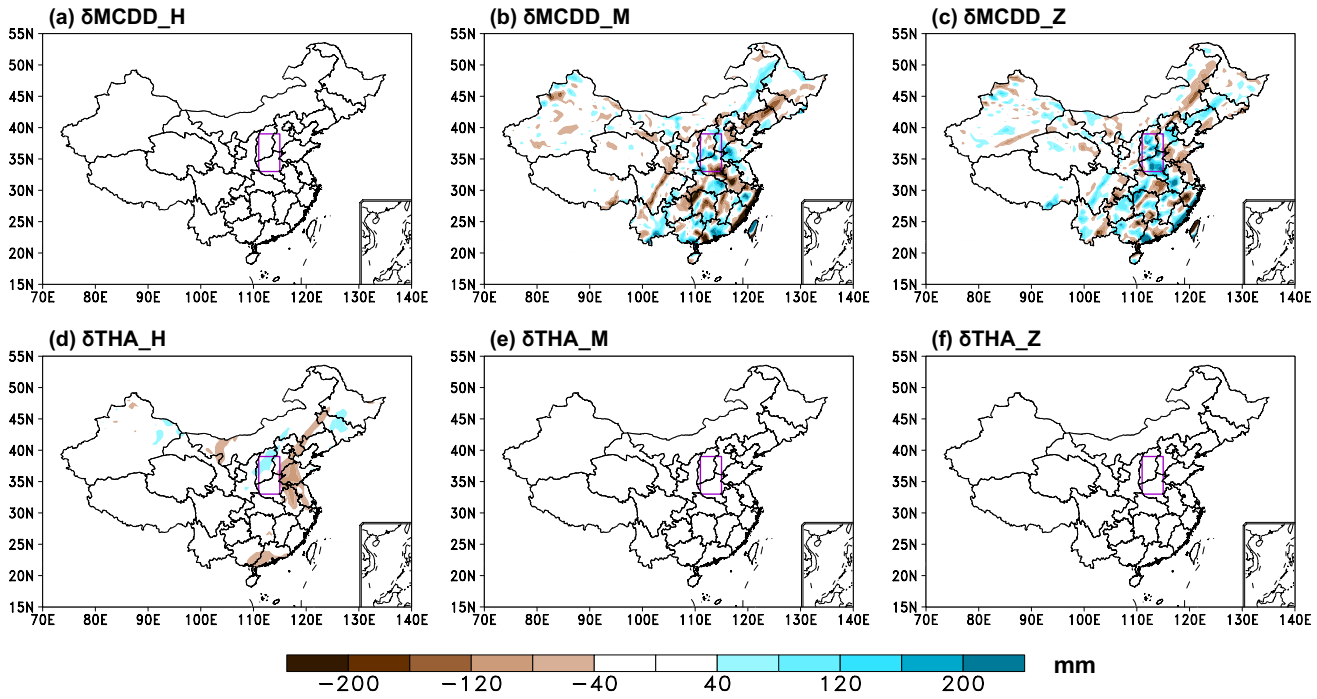

Fig. 3 The contributions of the change in divergence to the dynamic term induced by the (**a**) horizontal, (**b**) meridional, and (**c**) zonal circulations. (**d**)–(**f**) Same as (**a**)–(**c**) except for the contributions of changes in advection to the thermodynamic term induced by the (**d**) horizontal, (**e**) meridional, and (**f**) zonal circulations. The units for the changes in the moisture budget components are mm

residual term that includes the anomalous evaporation, high-frequency variability of transient eddies, nonlinear effects, and surface boundary terms (3.8 mm) only explains 3% of the anomalous precipitation, indicating that the dynamic and thermodynamic terms are the main contributors to the anomalous precipitation. Specifically, the regionally averaged δMCD and δTH are 94 mm and 27.7 mm, respectively, which can explain 75% and 22% of the anomalous precipitation. Figures 2b, d, and 4a (Figs. 2c, g, and 4a) show that the spatial distribution of δMCD (δTH) and that of δMCDD

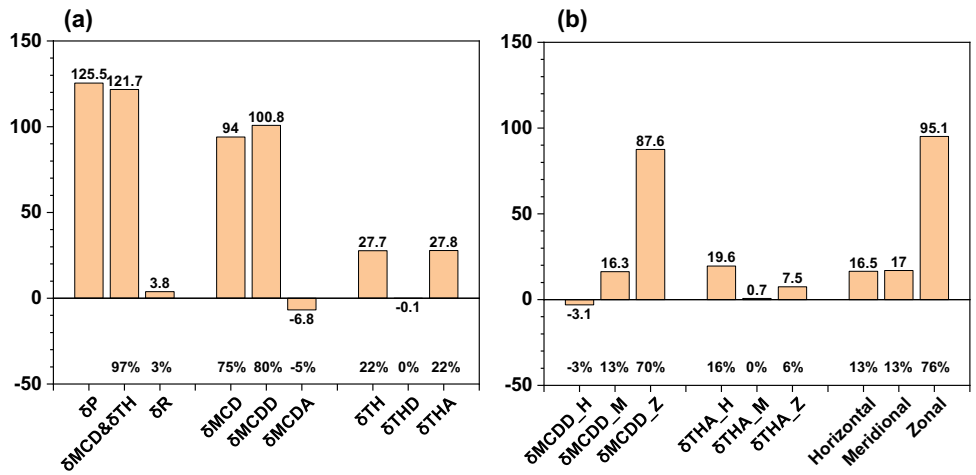

Fig. 4 **a** The regionally averaged precipitation anomaly over the region of the purple box (111°E–115°E, 33°N–39°N) and the calculated contributions of changes in the moisture budget components to the anomalous precipitation. (**b**) The calculated contributions of horizontal, meridional, and zonal circulations to the anomalous precipitation. The bars represent the regionally averaged precipitation anomaly derived from reanalysis datasets and the changes in the moisture budget components. The percentages are the ratios between changes in the moisture budget components and the precipitation anomaly derived from reanalysis datasets. The units for the precipitation anomaly and changes in the moisture budget components are mm

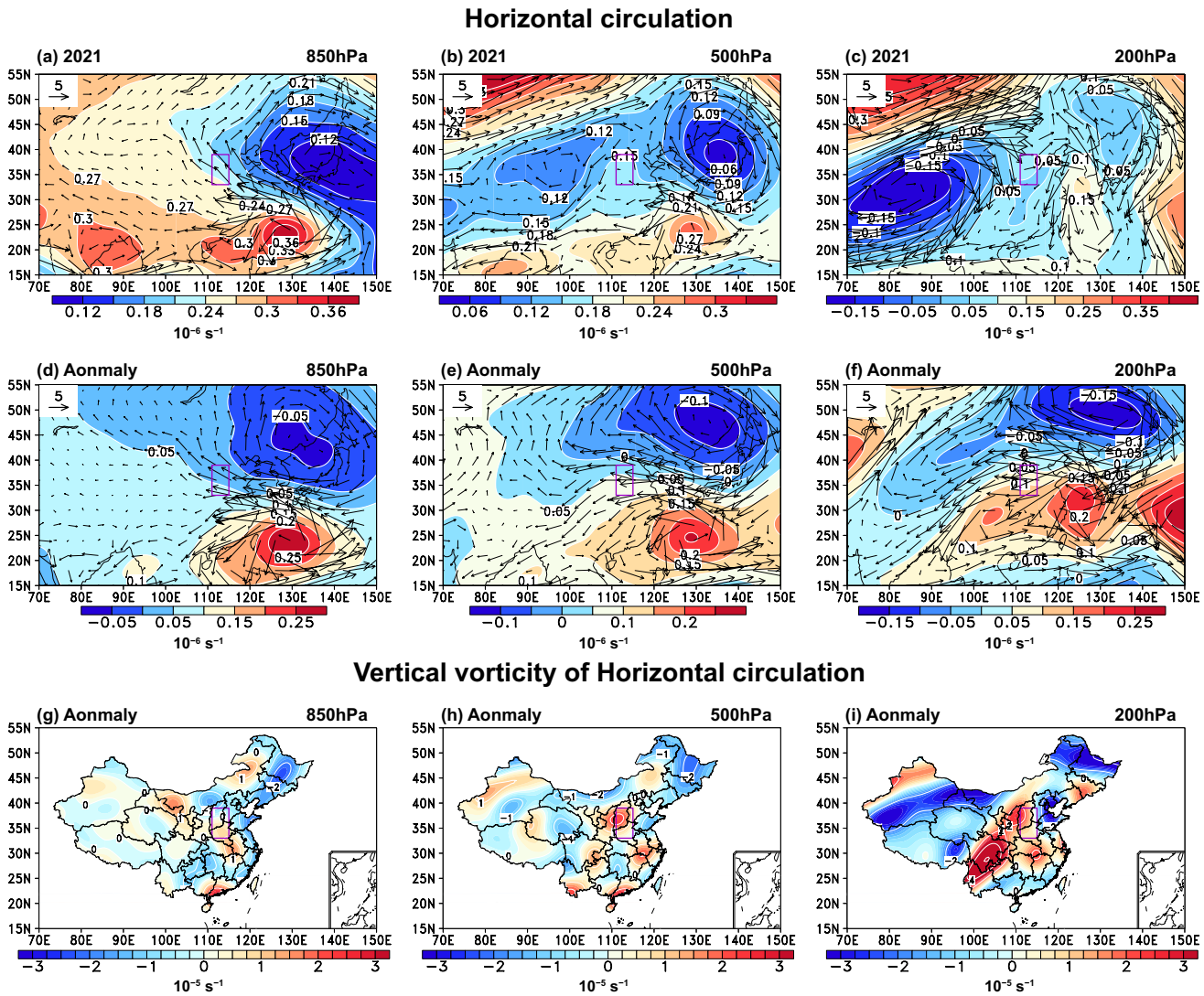

Fig. 5 Spatial distribution of the horizontal circulation at (**a**) 850 hPa, (**b**) 500 hPa, and (**c**) 200 hPa represented by the stream function (shading) and velocity fields (vectors) from 17 to 22 July in 2021. (**d**)–(**f**) Same as (**a**)–(**c**) except for the anomaly of horizontal circulation in 2021. (**g**)–(**i**) Spatial distribution of the vertical vorticity anomaly of horizontal circulation at (**g**) 850 hPa, (**h**) 500 hPa, and (**i**) 200 hPa. Anomalies are computed based on the climatological mean of 1981–2010. The units for the stream function, velocity fields, and vertical vorticity are 10^{-6} s^{-1}, m s^{-1}, and 10^{-5} s^{-1}

(δTHA) are similar in the region where the extreme precipitation occurs, and the regionally averaged δMCDD (δTHA) is 100.8 mm (27.8 mm), which can explain 80% (22%) of the anomalous precipitation, suggesting that changes in divergence (advection) are the main contributor to the dynamic (thermodynamic) term that further contributes to the anomalous precipitation.

To investigate the underlying physical mechanism, the contribution of the horizontal, meridional, and zonal circulations to δMCDD and δTHA was decomposed using the novel moisture budget equation of three-pattern circulations. Figure 3b,c shows that the contributions of meridional circulation and zonal circulation to δMCDD (δMCDD_M and δMCDD_Z) in the region where extreme precipitation occurs are positive, and δMCDD_Z is larger than δMCDD_M (Fig. 4). However, the contribution of horizontal circulation to δMCDD (δMCDD_H) is negligible (Fig. 3a). Specifically, the regionally averaged δMCDD_H, δMCDD_M, and δMCDD_Z are − 3.1 mm, 16.3 mm, and 87.6 mm, which can explain − 3%, 13%, and 70% of the anomalous precipitation (Fig. 4b). Figures 2g and 3d–f show that the spatial distribution of δTHA and that of the contribution of horizontal circulation to δTHA (δTHA_H) are similar, while the contributions of meridional circulation and zonal circulation to δTHA (δTHA_M and δTHA_Z) are small. Specifically, the regionally averaged δTHA_H, δTHA_M, and δTHA_Z are

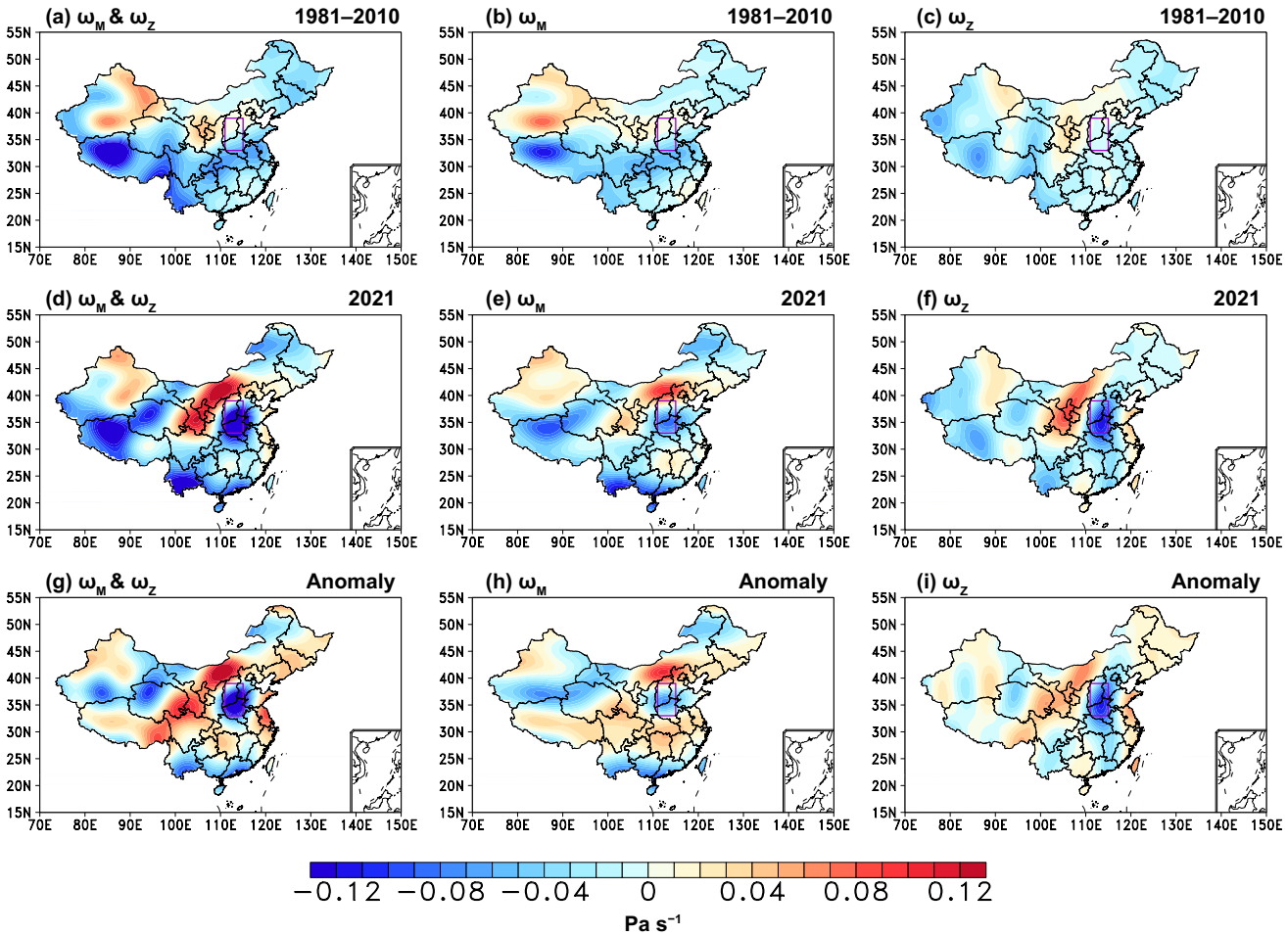

Fig. 6 Spatial distribution of the climatological (1981–2010) (**a**) omega of vertical circulation, (**b**) omega of meridional circulation, and (**c**) omega of zonal circulation at 500 hPa. (**d**)–(**f**) and (**g**)–(**i**) Same as (**a**)–(**c**) except for the omega and omega anomalies in 2021. The omega anomaly is computed based on the climatological mean of 1981–2010. The units for the omega and omega anomalies are Pa s^{-1}

19.6 mm, 0.7 mm, and 7.5 mm, which can explain 16%, 0%, and 6% of the anomalous precipitation (Fig. 4b). Generally, combining the results of δMCDD and δTHA reveals that the contributions of the horizontal, meridional, and zonal circulations to the anomalous precipitation caused by δMCDD and δTHA are 13%, 13%, and 76%, respectively (Fig. 4b), suggesting the dominant role of zonal circulation in causing this anomalous precipitation.

Figure 5a–f displays the spatial distribution of the horizontal circulation and the anomaly of horizontal circulation from 17 to 22 July in 2021. Figure 5a–c shows that typhoon "In-Fa" was formed in the northwest Pacific, which caused the low-pressure center in the northwest Pacific. The anomalous east wind caused by the convergence of typhoon "In-Fa" and the high-pressure center north of typhoon "In-Fa" can bring a large amount of water vapor from the northwest Pacific to the Chinese inland area, which can provide an abundant water vapor source for anomalous precipitation (Fig. 5d–f). The high-pressure center north of typhoon "In-Fa" and continental high caused two high-pressure centers in the middle latitudes at 500 hPa, which favored the formation of the inverted trough in the region where extreme precipitation occurs (Fig. 5b). In the upper troposphere, there also exists a low-pressure trough, and the region where extreme precipitation occurs is in front of the low-pressure trough at 200 hPa (Fig. 5c). Additionally, the anomalous vertical vorticity of the horizontal circulation from the lower troposphere to the upper troposphere is positive, which can provide dynamic lifting conditions for the anomalous precipitation (Fig. 5g–i).

The vertical motion was further induced under the background of the spatial distribution of the horizontal circulation (Fig. 6d). According to Eq. (3), the contribution of the meridional and zonal circulations to the vertical velocity can be decomposed using the 3P-DGAC method (Fig. 6).

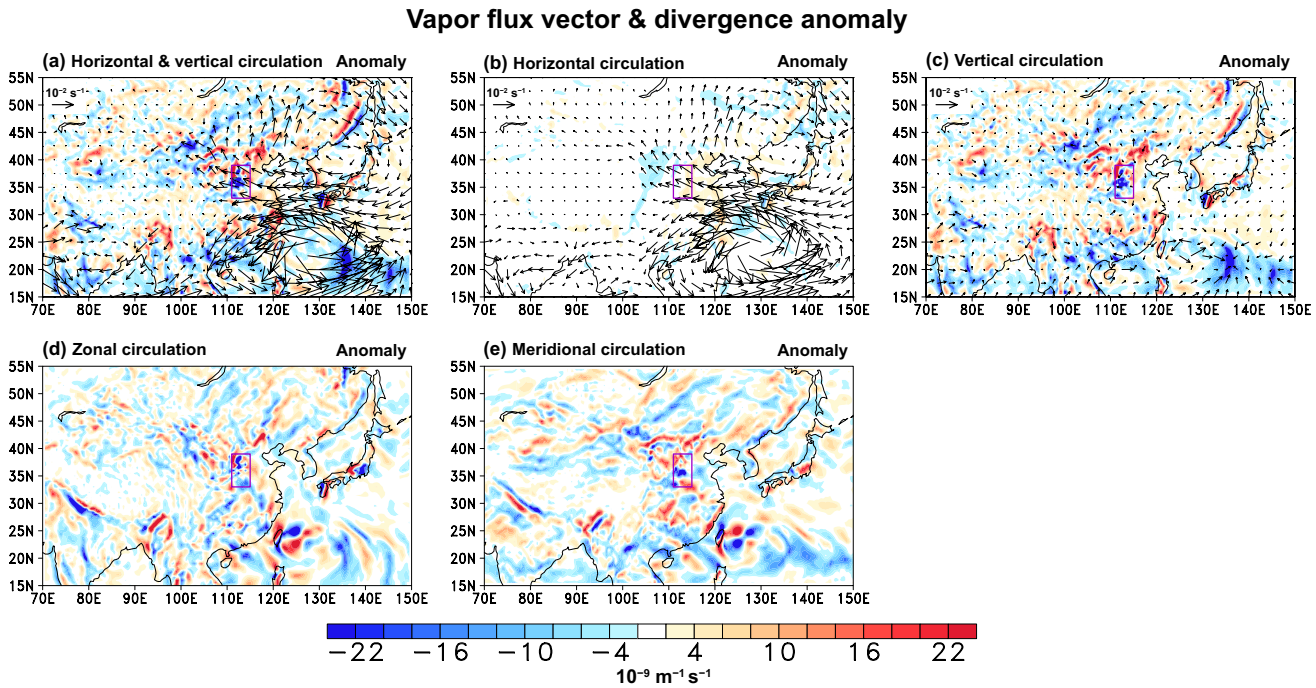

Fig. 7 **a** Spatial distribution of the vapor flux vector anomaly (vectors) and vapor flux divergence anomaly (shading) induced by the horizontal, meridional, and zonal circulations at 850 hPa in 2021. (**b**) and (**c**) Same as (**a**) except for the vapor flux vector anomaly and vapor flux divergence anomaly induced by the horizontal circulation and the vertical circulation. (**d**) and (**e**) Same as (**a**) except for the vapor flux divergence anomaly induced by zonal circulation and meridional circulation. Anomalies are computed based on the climatological mean of 1981–2010. The units for the vapor flux vector anomaly and vapor flux divergence anomaly are 10^{-2} s^{-1} and 10^{-9} m^{-1} s^{-1}, respectively

Namely, the vertical velocity ω can be decomposed into the sum of the vertical velocity of the meridional circulation (ω_M) and zonal circulation (ω_Z). In terms of climatic mean, the spatial distributions of ω and ω_M are similar, and the regionally averaged ω, ω_M, and ω_Z are -0.015 Pa s^{-1}, -0.012 Pa s^{-1}, and -0.003 Pa s^{-1}, implying that meridional circulation plays the dominant role in the climatic mean (Fig. 6a–c). In 2021, the regionally averaged ω was -0.126 Pa s^{-1} (Fig. 6d), which is an order of magnitude greater than the climatic mean. Additionally, the regionally averaged ω_Z (-0.082 Pa s^{-1}) was about twice as large as the ω_M (-0.044 Pa s^{-1}) in 2021 (Fig. 6e,f), and the anomalies of the regionally averaged ω, ω_M, and ω_Z are -0.111 Pa s^{-1}, -0.032 Pa s^{-1}, and -0.079 Pa s^{-1}, respectively, suggesting that zonal circulation plays the dominant role, which is different from the climatic mean.

Figure 7 displays the spatial distribution of the vapor flux vector anomaly and vapor flux divergence anomaly induced by the horizontal, meridional, and zonal circulations at 850 hPa in 2021. The spatial distributions of the vapor flux vector anomaly in Fig. 7a,b are almost identical, and the vapor flux vector anomaly induced by the vertical circulation (The vertical circulation includes the meridional and zonal circulations) is tiny (Fig. 7c), implying that horizontal circulation plays a dominant role in bringing water vapor from the northwest Pacific to the Chinese inland area. Although horizontal circulation plays the dominant role in the transport of vapor flux, the contribution of horizontal circulation to the anomalous precipitation is 13% (Fig. 4b). This is because whether precipitation can be formed depends on the vapor flux divergence anomaly rather than the vapor flux vector anomaly. The vapor flux divergence anomaly in the region where extreme precipitation occurs is negative (Fig. 7a), indicating the convergence of water vapor, which is beneficial to anomalous precipitation. The spatial distributions of the vapor flux divergence anomaly in Fig. 7a,c are almost identical, and the vapor flux divergence anomaly induced by the horizontal circulation is tiny (Fig. 7b). Additionally, the vapor flux divergence anomaly in the region where extreme precipitation occurs induced by zonal circulation (-2.6×10^{-9} m^{-1} s^{-1}) is approximately two and a half times that induced by meridional circulation (-1.0×10^{-9} m^{-1} s^{-1}), which is consistent with the results that zonal circulation plays the dominant role (Fig. 4b).

4 Summary

In this study, we analyzed the extreme precipitation in Henan Province from 17 to 22 July 2021 by using the moisture budget equation and the 3P-DGAC method. The following conclusions are obtained.

(1) δMCD and δTH can explain 75% and 22% of the anomalous precipitation, respectively, while the residual term only explains 3%. Changes in divergence (advection) are the main contributor to the δMCD (δTH), which can explain 80% (22%) of the anomalous precipitation.

(2) The typhoon "In-Fa," anomalous high-pressure center north of typhoon "In-Fa," continental high, and low-pressure trough provide abundant water vapor sources and dynamic lifting conditions for anomalous precipitation.

(3) Since precipitation formation relates to the vapor flux divergence anomaly rather than the vapor flux vector anomaly, although horizontal circulation can bring water vapor from the northwest Pacific to the Chinese inland area, the contribution of horizontal circulation to anomalous precipitation is only 13%. In contrast, zonal circulation, which is the main contributor to the vapor flux divergence anomaly, can explain 76% of the anomalous precipitation, while meridional circulation can explain 13%.

Author contribution All authors contributed to the study conception and design. JC performed the analysis and wrote the manuscript. YZ performed the analysis. RZ revised the manuscript. GF provided guidance and revised the manuscript.

Funding This work was funded by the National Natural Science Foundation of China (42130610, 42005012, 41975088), the Natural Science Foundation of Jiangsu Province (BK20201058), the National Key Research and Development Program of China (2017YFC1502303), and the School-level research projects of Yancheng Institute of Technology (xjr2020022).

Data availability The hourly rainfall data and atmospheric variables from ERA5 data were available at https://cds.climate.copernicus.eu/cdsapp#!/search?text=ERA5&type=-dataset.

Code availability The code analyzed during the current study are available from the corresponding author on reasonable request.

Declarations

Ethics approval Not applicable.

Consent to participate Not applicable.

Consent for publication Not applicable.

Conflict of interest The authors declare no competing interests.

References

Cheng J, Gao C, Hu S, Feng G (2018) High-stability algorithm for the three-pattern decomposition of global atmospheric circulation. Theor Appl Climatol 133:851–866. https://doi.org/10.1007/s00704-017-2226-2

Han Z, Su T, Zhang Q, Wen Q, Feng G (2019a) Thermodynamic and dynamic effects of increased moisture sources over the Tropical Indian Ocean in recent decades. Clim Dyn 53:7081–7096. https://doi.org/10.1007/s00382-019-04977-w

Han Z, Su T, Huang B, Feng T, Qu S, Feng G (2019b) Changes in global monsoon precipitation and the related dynamic and thermodynamic mechanisms in recent decades. Int J Climatol 39:1490–1503. https://doi.org/10.1002/joc.5896

Han Z, Zhang Q, Wen Q, Lu Z, Feng G, Su T, Li Q, Zhang Q (2020) The changes in ENSO-induced tropical Pacific precipitation variability in the past warm and cold climates from the EC-Earth simulations. Clim Dyn 55:503–519. https://doi.org/10.1007/s00382-020-05280-9

Han Z, Zhang Q, Li Q, Feng R, Haywood AM, Tindall JC et al (2021) Evaluating the large-scale hydrological cycle response within the Pliocene Model Intercomparison Project Phase 2 (PlioMIP2) ensemble. Clim past 17:2537–2558. https://doi.org/10.5194/cp-17-2537-2021

Hersbach H, Bell B, Berrisford P, Hirahara S, Horányi A, Muñoz-Sabater J et al (2020) The ERA5 global reanalysis. Q J Roy Meteor Soc 146:1999–2049. https://doi.org/10.1002/qj.3803

Hu S, Cheng J, Chou J (2017) Novel three-pattern decomposition of global atmospheric circulation: generalization of traditional two dimensional decomposition. Clim Dyn 49:3573–3586. https://doi.org/10.1007/s00382-017-3530-3

Hu S, Chou J, Cheng J (2018a) Three-pattern decomposition of global atmospheric circulation: part I—decomposition model and theorems. Clim Dyn 50:2355–2368. https://doi.org/10.1007/s00382-015-2818-4

Hu S, Cheng J, Xu M, Chou J (2018b) Three-pattern decomposition of global atmospheric circulation: part II—dynamical equations of horizontal, meridional and zonal circulations. Clim Dyn 50:2673–2686. https://doi.org/10.1007/s00382-017-3763-1

Hu S, Zhou B, Gao C, Xu Z, Chou J (2020) Theory of three-pattern decomposition of global atmospheric circulation. Sci China Earth Sci 63:1248–1267. https://doi.org/10.1007/s11430-019-9614-y

Liu H, Hu S, Xu M, Chou J (2008) Three-dimensional decomposition method of global atmospheric circulation. Sci China Ser D 51:386–402. https://doi.org/10.1007/s11430-008-0020-9

Qiao S, Chen D, Wang B, Cheung HN, Liu F, Cheng J, Tang S, Zhang Z, Feng G, Dong W (2021) The longest 2020 Meiyu season over the past 60 years: subseasonal perspective and its predictions. Geophys Res Lett 48:e2021GL093596. https://doi.org/10.1029/2021GL093596

Seager R, Naik N, Vecchi GA (2010) Thermodynamic and dynamic mechanisms for large-scale changes in the hydrological cycle in response to global warming. J Clim 23:4651–4668. https://doi.org/10.1175/2010JCLI3655.1

Seager R, Vecchi GA (2010) Greenhouse warming and the 21st century hydroclimate of southwestern North America. Proc Natl Acad Sci USA 107:21277–21282. https://doi.org/10.1073/pnas.0910856107

Shi W, Li X, Zeng M, Zhang B, Wang H, Zhu K, Zhu X (2021) Multi-model comparison and high-resolution regional model forecast analysis for the "7·20" Zhengzhou severe heavy rain. Transactions of Atmospheric Sciences 44: 688–702. https://doi.org/10.13878/j.cnki.dqkxxb.20210823001 (in Chinese)

Sun Y, Xiao H, Yang H, Ding J, Fu D, Guo X, Feng L (2021) Feature analysis of dynamic condition and hydrometeor transportation among Zhengzhou "7·20" superheavy rainfall event based on optical flow field of remote sensing data. Chin J Atmos Sci 45:1384–1399. https://doi.org/10.3878/j.issn.1006-9895.2109.21155 ((inChinese))

Yin J, Gu H, Liang X, Yu M, Sun J, Xie Y, Li F, Wu C (2021) A possible dynamic mechanism for rapid production of the extreme hourly rainfall in Zhengzhou city on 20 July 2021. J Meteorol Res. https://doi.org/10.1007/s13351-022-1166-7

Zhang X, Yang H, Wang X, Shen L, Wang D, Li H (2021) Analysis on characteristic and abnormality of atmospheric circulations of the July 2021 extreme precipitation in Henan. Trans Atmos Sci 44:672–687. https://doi.org/10.13878/j.cnki.dqkxxb.20210907001 ((in Chinese))